Rapid Communications

# Implications of the $^{36}$Ca-$^{36}$S and $^{38}$Ca-$^{38}$Ar difference in mirror charge radii on the neutron matter equation of state

B. A. Brown,[1,2] K. Minamisono,[1,2] J. Piekarewicz,[3] H. Hergert,[1,2] D. Garand,[1] A. Klose,[4] K. König,[1] J. D. Lantis,[1,5] Y. Liu,[6] B. Maaß,[7] A. J. Miller,[1,2] W. Nörtershäuser,[7] S. V. Pineda,[1,5] R. C. Powel,[1,2] D. M. Rossi,[7] F. Sommer,[7] C. Sumithrarachchi,[1] A. Teigelhöfer,[8] J. Watkins,[1,2] and R. Wirth[1]

[1]*National Superconducting Cyclotron Laboratory, Michigan State University, East Lansing, Michigan 48824, USA*
[2]*Department of Physics and Astronomy, Michigan State University, East Lansing, Michigan 48824, USA*
[3]*Department of Physics, Florida State University, Tallahassee, Florida 32306, USA*
[4]*Department of Chemistry, Augustana University, Sioux Falls, South Dakota 57197, USA*
[5]*Department of Chemistry, Michigan State University, East Lansing, Michigan 48824, USA*
[6]*Facility for Rare Isotope Beams, Michigan State University, East Lansing, Michigan 48824, USA*
[7]*Institut für Kernphysik, Technische Universität Darmstadt, 64289 Darmstadt, Germany*
[8]*TRIUMF, Vancouver, BC V6T 2A3, Canada*

(Received 28 February 2020; accepted 21 April 2020; published 11 May 2020)

Charge radii of the unstable $^{36}$Ca and $^{38}$Ca nuclei were recently determined and used to compute differences in charge radii between mirror nuclei $\Delta R_{\rm ch}$ for the $^{36}$Ca-$^{36}$S and $^{38}$Ca-$^{38}$Ar mirror pairs. Given the correlation between $\Delta R_{\rm ch}$ and the slope of the symmetry energy $L$ at the nuclear saturation density, we deduce $L = 5$–$70$ MeV, which rules out a large fraction of models that predict a "stiff" equation of state. This is the most precise determination of $L$ in this model based on electromagnetic probes of nuclear ground states. The determined range is consistent with earlier analyses from both laboratory experiments and astrophysical observations, including the recent detection of gravitational waves from the merger of two neutron stars.

DOI: 10.1103/PhysRevResearch.2.022035

## I. INTRODUCTION

The slope of the symmetry energy $L$ at the saturation nucleon density is critical for guiding the extrapolation to both lower and higher densities [1], as required for the predictions of the properties of superheavy nuclei as well as for the understanding of neutron stars [2,3]. As a matter of fact, the recent detection of the gravitational wave from the neutron star merger GW170817 [4] set some constraints on the equation of state of the neutron-rich matter [5]. Given that symmetric nuclear matter saturates, $L$ is closely related to the pressure of pure neutron matter at the saturation nucleon density $\rho_0 = 0.16$ nucleons/fm$^3$. Although $L$ cannot be directly measured in the laboratory, the neutron skin $\Delta R_{\rm np}$ of neutron-rich nuclei, such as $^{208}$Pb and $^{48}$Ca, is known to be strongly correlated to $L$ [6]. Here the $\Delta R_{\rm np}$ is defined as the difference between the neutrons and protons root-mean-square radii.

Assuming perfect charge symmetry, the neutron radius of a given nucleus is equal to the proton radius of its corresponding mirror nucleus. The $\Delta R_{\rm np}$ can then be obtained from the difference $\Delta R_{\rm ch}$ of root-mean-square charge radii $R_{\rm ch}$ of the mirror nuclei [7,8] as

$$\Delta R_{\rm np} = R_{\rm ch}\left({}^{A}_{Z}X_N\right) - R_{\rm ch}\left({}^{A}_{N}Y_Z\right) = \Delta R_{\rm ch}, \qquad (1)$$

where $A$ is the mass number $A = N + Z$, and $N$ and $Z$ are the neutron and proton numbers, respectively. In reality, however, charge symmetry is broken by the Coulomb interaction that pushes out protons relative to neutrons, leading to a weaker correlation between $\Delta R_{\rm np}$ and $\Delta R_{\rm ch}$. The result is that $\Delta R_{\rm ch}$ is strongly correlated with $|N - Z| \times L$ even when $|N - Z|$ is small. On the other hand, $\Delta R_{\rm np}$ depends on both $|N - Z| \times L$ and the symmetry energy with the $L$ dependence dominating at large $|N - Z|$ [7]. Thus, $\Delta R_{\rm ch}$ provides a clean (purely electromagnetic) alternative to the parity-violating asymmetry [9] and the electric dipole polarizability [10–13] in constraining the density dependence of the symmetry energy.

For mirror pairs with large $|N - Z|$, most of the proton-rich partners lie near the proton drip line, whereas the corresponding neutron-rich partners are stable or near stable, e.g., the $^{48}$Ni-$^{48}$Ca pair. While the symmetry energy impacts both proton- and neutron-rich nuclei, the added Coulomb repulsion among protons severely limits the number of bound proton-rich nuclei. Therefore, measuring charge radii of proton-rich nuclei is experimentally challenging and no pair is currently available with $|N - Z| > 4$, whose charge radii are both known [14].

In the present study the $\Delta R_{\rm ch}$ for the pairs of $^{36}$Ca-$^{36}$S and $^{38}$Ca-$^{38}$Ar were evaluated using recently determined $R_{\rm ch}$ of proton-rich nuclei $^{36,38}$Ca [15]. The mirror partners $^{36}$S and $^{38}$Ar are stable nuclei, and their $R_{\rm ch}$ are well known [16]. The $A = 36$ and 38 mirror pairs provide a unique opportunity to investigate the correlation between $L$ and $\Delta R_{\rm ch}$. The $A = 36$ pair has the largest $|N - Z| = 4$ of any known mirror $R_{\rm ch}$ pairs so far and the $A = 38$ pair is known with much higher

TABLE I. $R_{ch}$ and $\Delta R_{ch}$ for the $A = 36$ and 38 pairs. The first and second parentheses on the value of charge radii are for statistical and systematic uncertainties, respectively, whose quadratic sum was used for the uncertainty of $\Delta R_{ch}$.

| $A$ | | $R_{ch}$ (fm) | $\Delta R_{ch}$ (fm) |
|---|---|---|---|
| 36 | Ca | 3.4484(32)(27) | |
| | S | 3.2982(09)(12) | 0.150(4) |
| 38 | Ca | 3.4652(09)(17) | |
| | Ar | 3.4022(10)(15) | 0.063(3) |
| 40 | Ca | 3.4767(09)(14) | |

precision than the $A = 36$, giving the highest sensitivity to determine $L$.

## II. EXPERIMENTAL RADII

$R_{ch}$ and $\Delta R_{ch}$ for the relevant mirror partners are listed in Table I. $R_{ch}$ of stable isotopes $^{36}$S, $^{38}$Ar, and $^{40}$Ca were obtained from a combined analysis of elastic electron scattering data and transition energies of muonic atoms [16]. Model-independent Barrett equivalent radii [17] were converted to $R_{ch}$ using a ratio $V_2$ between Barrett moment and a radial moment determined from elastic electron scattering data. These $R_{ch}$ of stable isotopes are known to better than 0.1%. It is noted that the $R_{ch}(^{38}\mathrm{Ar})$ was obtained using a ratio of radial moments $V_2$ evaluated by an interpolation of those between $^{36,40}$Ar [16], but the influence on the present discussion is negligible. For $^{36}$S, the $V_2$ values are obtained from [18].

We determined [15] the differential mean-square charge radii $\delta\langle r^2\rangle^{A,A'} = R^{A'}_{ch} - R^{A}_{ch}$ relative to $^{40}$Ca as $\delta\langle r^2\rangle^{40,36} = -0.196(21)(16)$ fm$^2$ for $^{36}$Ca and $\delta\langle r^2\rangle^{40,38} = -0.0797(11)(63)$ fm$^2$ for $^{38}$Ca, where the first and second parentheses denote statistical and systematic uncertainties, respectively. The $R_{ch}$ of $^{36,38}$Ca were then evaluated as $R^2_{ch}(^A\mathrm{Ca}) = R^2_{ch}(^{40}\mathrm{Ca}) + \delta\langle r^2\rangle^{40,A}$ with the $\delta\langle r^2\rangle^{40,A}$ of $^{36,38}$Ca and the $R_{ch}$ of $^{40}$Ca discussed above.

It is noted that $R_{ch}$ of $^{37,39}$Ca were also determined in Ref. [15]. The radii of their stable mirror partners $^{37}$Cl and $^{39}$K, respectively, are evaluated [16] to be used for $\Delta R_{ch}$. However, the experimental uncertainty of $\Delta R_{ch}$ is large for the $A = 37$ pair, and the $A = 39$ pair is less sensitive to $L$ due to the small $|N - Z|$ than the $A = 36$ and 38 pairs. Also the combined analysis cannot be used for the evaluation of $R_{ch}$ [16] due to the lack of muonic atom data for $^{37}$Cl and electron scattering data for $^{39}$K, and no reliable values of $R_{ch}$ for $^{37}$Cl and $^{39}$K are available. Therefore the results on $\Delta R_{ch}$ for the $A = 37$ and 39 pairs are not discussed here.

## III. THEORETICAL RADII

The results for $\Delta R_{ch}$ are plotted as a function of $L$ in Fig. 1. A set of 48 Skyrme energy density functionals (EDFs) was used [7] to predict the correlation between $\Delta R_{ch}$ and $L$, and is shown by the colored filled circles in Fig. 1. Starting with an original set of 12 Skyrme EDFs [19], their isovector properties were modified to give specific values for the presently unknown neutron skin of $^{208}$Pb: 0.12 fm (red), 0.16 fm (orange), 0.20 fm (green), and 0.24 fm (blue). The black dots are the set of 12 Skyrme EDFs with the additional constraints that the EDFs reproduce *ab initio* calculations for the low-density neutron equation of state and the maximum mass of neutron stars of about 2.1 solar masses [20].

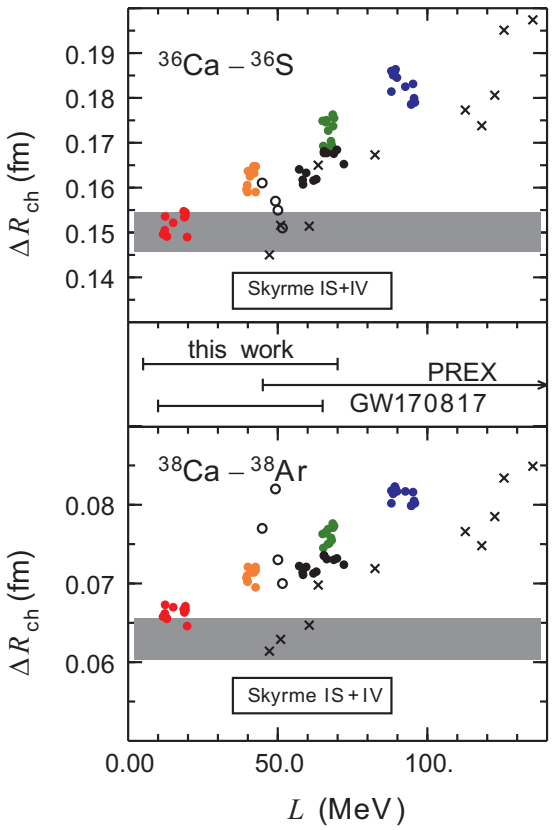


FIG. 1. $\Delta R_{ch}$ as a function of $L$ at $\rho_0$. The experimental results are shown as a horizontal band. The solid circles are results of Skyrme EDF, the crosses are from the CODF, and the open circles are from IMSRG calculations. Details of these calculations are described in the text. Note the difference of the scale for the $\Delta R_{ch}$ axes. The isoscalar plus isovector (IS + IV) form was used for the spin-orbit potential.

Also shown with crosses in Fig. 1 are predictions from covariant density functional (CODF) theory where a correlation between $\Delta R_{ch}$ and $L$ was also found [8]. Covariant density functional theory aims to build high-quality functionals that yield an accurate description of the properties of finite nuclei, generate an equation of state that is consistent with known neutron-star properties while providing a Lorentz covariant extrapolation to dense matter. To assess uncertainties in the model predictions and in particular on the density dependence of the symmetry energy, a comprehensive set of modern covariant density functionals was used; they are listed in Table II in order of increasing $L$ values. Among them, NL3 [21,22], FSUGold [23], and IU-FSU [24] have been used extensively in the literature. Besides these functionals, we employ the TAMU-FSU set that is characterized by a relatively stiff symmetry energy that was used to explore whether the existence of thick neutron skins in $^{208}$Pb could already be ruled out by experiment [25]. The remaining covariant density functionals were calibrated for the first time using exclusively

TABLE II. Models used for the calculation of $R_{ch}$. The values of $L$ are given with the $\Delta R_{ch}$ for $A = 36$ and $R_{ch}$ for $^{36}$Ca.

| Type | Name | $L$ (MeV) | $\Delta R_{ch}$ (fm) | $R_{ch}$ (fm) |
|---|---|---|---|---|
| CODF | IUFSU | 47.2 | 0.145 | 3.414 |
| | FSUGarnet | 50.9 | 0.152 | 3.418 |
| | FSUGold | 60.5 | 0.151 | 3.432 |
| | RMF022 | 63.5 | 0.165 | 3.431 |
| | TAMUFSUa | 82.5 | 0.167 | 3.446 |
| | FSUGold2 | 112.7 | 0.177 | 3.449 |
| | NL3 | 118.2 | 0.174 | 3.458 |
| | TAMUFSUb | 122.5 | 0.181 | 3.461 |
| | RMF032 | 125.6 | 0.195 | 3.451 |
| | TAMUFSUc | 135.2 | 0.197 | 3.477 |
| IMSRG | EM2.0/2.0 (PWA) | 44.8 | 0.161 | 3.509 |
| | EM2.2/2.0 | 49.2 | 0.157 | 3.336 |
| | EM2.0/2.0 | 50.1 | 0.155 | 3.309 |
| | EM1.8/2.0 | 51.6 | 0.151 | 3.270 |

genuine physical observables without any reliance on bulk properties of infinite nuclear matter [26,27]. The fitting protocol involved a robust covariance analysis that provided both theoretical uncertainties and correlation coefficients [26]. The only difference in the calibration of this set of functionals was an assumed value for the presently unknown neutron skin thickness of $^{208}$Pb, which in turn provides a wide range of values for $L$ [26]. We note that the covariant EDFs presented here, while representative of the field, are not comprehensive. Results from other covariant EDFs, primarily those involving a density-dependent coupling constant [28], were not included in the present study.

We have also computed $R_{ch}$ using the multireference in-medium similarity renormalization group (IMSRG) approach [29–31], using a family of chiral interactions [32] that is commonly denoted by EM$\lambda/\Lambda$. They consist of Entem and Machleidt's two-nucleon interaction at next-to-next-to-next-to-leading order (N3LO) in the chiral expansion, evolved to a lower resolution scale $\lambda$, and a next-to-next-to-leading order (N2LO) three-nucleon interaction with cutoff $\Lambda$. The 3N interaction's low-energy constants (LECs) $c_D$ and $c_E$ are fitted to the triton binding energy and the charge radius of $^4$He, while the LECs of the long-range terms are either chosen consistently with the NN interaction, or extracted from the Nijmegen partial wave analysis [EM2.0/2.0 (PWA)] [32]. The $\Delta R_{ch}$ are shown as open circles in Fig. 1. The nuclear matter results for these Hamiltonians are from Ref. [33].

The results are summarized in Table II, where a systematic ∼10% variation with the cutoff parameters can be seen that matches a comparable variation in the ground-state energies [34]. Empirically, the EM1.8/2.0 interaction provides excellent agreement between IMSRG ground-state energies and data through at least the $A \sim 60$–70 region [34,35], but underpredicts experimental charge radii. The scatter of the charge radii from CODF (shown for comparison in Table II), and Skyrme functionals, which give $R_{ch}$ from 3.44 to 3.53 fm, is significantly smaller than the IMSRG results. Since the IMSRG produces systematic offsets between (known) measured and computed charge radii, these offsets cancel in radius differences and results for $\Delta R_{ch}$ are robust and comparable to those for CODF and Skyrme functionals.

We find some correlation of $R_{ch}$ and $L$ for the IMSRG results, while no correlation is evident in the CODF and Skyrme results. We note, however, that there is a relatively large uncertainty in the absolute radii due to the additional isoscalar parameters of the models, which mostly cancels in $\Delta R_{ch}$.

In all of the theoretical models, what is actually computed is the "point proton" density from which the point proton radius $R_p$ is extracted. The charge radius is then obtained from $R_p$ by adding corrections that account for the finite charge size of both protons and neutrons as well as relativistic corrections. That is, $R_{ch}^2 = R_p^2 + r_p^2 + (N/Z)\, r_n^2 + r_{rel}^2$, where $r_p$ and $r_n$ are the mean-square charge radii for proton [36] and neutron [37]: $r_p = 0.8414(19)$ fm and $r_n^2 = -0.116(2)$ fm$^2$. Note that for $r_p$ we have adopted the 2018 CODATA recommended value, which is significantly smaller than the previously recommended CODATA value of $r_p = 0.8775(51)$ fm, due to the inclusion of a very precise value obtained from the measurement of the Lamb shift in muonic hydrogen [38]. This difference for $r_p$ would increase the calculated $R_{ch}$ by 0.009 fm and increase the $\Delta R_{ch}$ by only 0.001 fm, both negligible as compared to the theoretical model-dependent uncertainties. However, the understanding of the "proton radius puzzle" may have some impact on the interpretation of $R_{ch}$ determined in experiments. For our results we rely on atomic experiments for $^{36,38}$Ca and muonic-atom results for $^{36}$S, $^{38}$Ar, and $^{40}$Ca. Note that recent measurements in hydrogen [39,40] as well as a recent electron scattering experiment [41] are now consistent with the smaller $r_p$ obtained from muonic hydrogen.

The relativistic correction $r_{rel}$ has its origin in the tensor component of the electromagnetic current, which has been explicitly computed in the CODF formalism in Ref. [42]. The same correction has been included in the Skyrme EDF results, including the approximate 30% enhancement predicted by the CODF approach due to the in-medium modification of the effective nucleon mass [42]. In the IMSRG, we evaluate the operators that give rise to the relativistic corrections [43] consistently alongside $r_p$ and $r_n$ [34]. In all the theoretical models the structure of $^{36}$Ca is dominated by shell-model configurations, where the $0d_{3/2}$ orbital is filled for protons and empty for neutrons. The opposite situation happens in the case of its mirror nucleus $^{36}$S. Relativistic corrections induce a relatively large downward shift of 0.018 to 0.020 fm for the $A = 36$ pair, which is four times larger than the experimental uncertainty. The relativistic corrections for the $A = 38$ pair is about half of that for the $A = 36$ pair.

## IV. DISCUSSION

Constraints on $L$ are deduced by comparing theoretical predictions with the experimental results in Fig. 1. Note that the results for $A = 36$ and $A = 38$ provide a consistent picture. In the simplest approximation, the $\Delta R_{ch}$ for the $A = 36$ pair would be twice as large as those for the $A = 38$ pair. However, the $\Delta R_{ch}(A = 36)$ to $\Delta R_{ch}(A = 38)$ ratio is closer to 2.3 for experiment and for most of the theoretical predictions. This comes from the fact that protons are in general less bound in

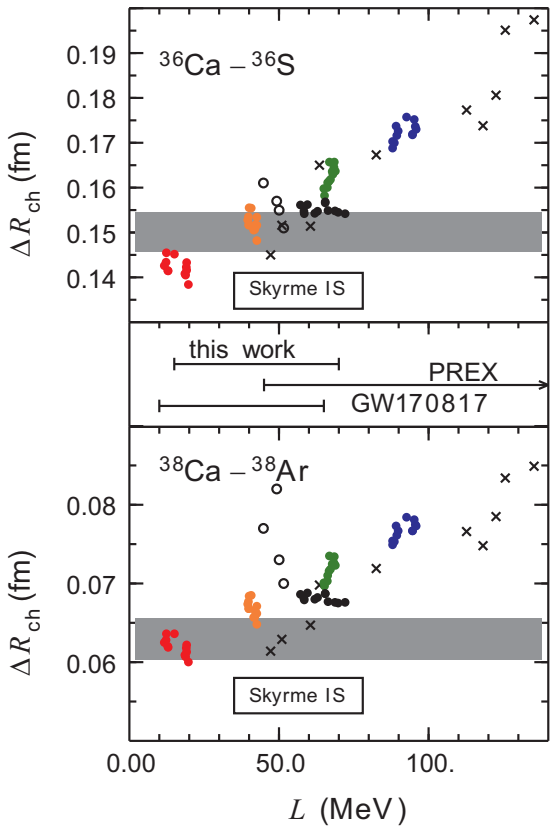


FIG. 2. $\Delta R_{ch}$ as a function of $L$ at $\rho_0$. Same as Fig. 1, except that the isoscalar (IS) form was used for the Skyrme spin-orbit potential.

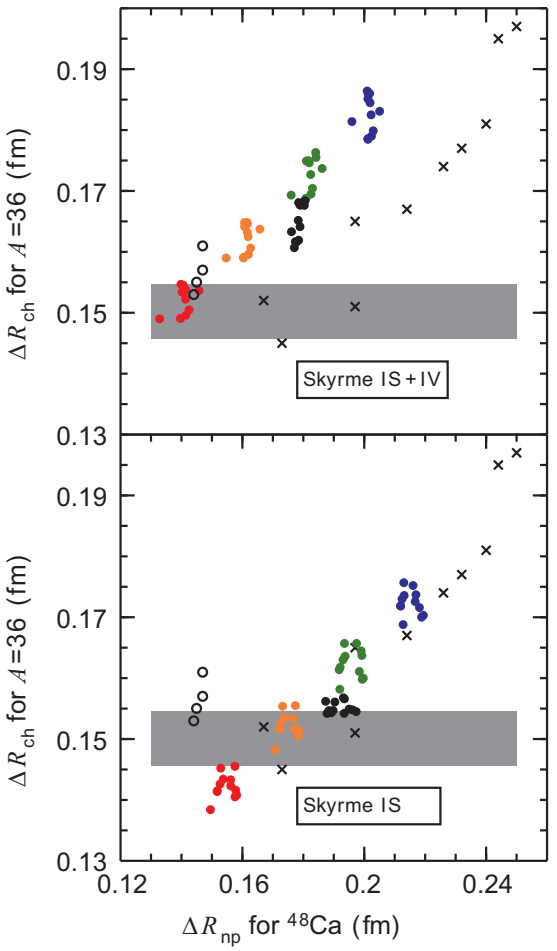


FIG. 3. The correlation between $\Delta R_{ch}$ for $A = 36$ and the neutron skin of $^{48}$Ca. The symbols are the same as in Figs. 1 and 2.

$^{36}$Ca than in $^{38}$Ca. Indeed, $^{36}$Ca with a relatively large radius lies close to the proton continuum [15].

The Skyrme and CODF results display an approximate linear correlation between $\Delta R_{ch}$ and $L$ as expected from [7]. However, there is about a 0.10 fm offset between the Skyrme and CODF results. This difference can be traced back to the functional form used for the spin-orbit potential. The Skyrme potential is obtained from $p$-wave interaction that results in a single-particle spin-orbit potential that is proportional to $2J_p + J_n$ for protons and $J_p + 2J_n$ for neutrons [44], where $J_p$ is the spin-orbit potential coming from the proton density, and $J_n$ coming from the neutron density. This potential contains both isoscalar and isovector parts denoted by (IS + IV). However, in the CODF formalism the spin-orbit potential is dominated by just the isoscalar (IS) form proportional to $J_p + J_n$ for both protons and neutrons. The isospin contributions largely come from isoscalar-scalar ("sigma") and isoscalar-vector ("omega") mesons, which results in a very strong split-orbit interaction. There is also an isovector component from "rho" exchange but this is small, especially in the case of nuclei with a small neutron-proton asymmetry. The difference between the Skyrme and CODF forms leads to some changes in the isotope shifts [45,46]. We redid the Skyrme calculations with the isoscalar form (with its strength adjusted to reproduce the spin-orbit splittings). The results are shown in Fig. 2. Now the Skyrme and CODF results are consistent.

The correlation between $\Delta R_{ch}$ for the $A = 36$ pair and $\Delta R_{np}$ in $^{48}$Ca is depicted in Fig. 3. This shows the complementary aspects of the $R_{ch}$ experiments and the parity-violating asymmetry experiments at JLab for the $R_{np}$. The top panel shows the results with the $p$-wave form (IS + IV) of the Skyrme spin-orbit potential used in Fig. 1. The bottom panel shows the results with the IS form of the Skyrme spin-orbit potential used in Fig. 2. The origin of the shift is that the spin-orbit potential is opposite in sign for the $0d_{3/2}$ ($A = 36$) and the $0f_{7/2}$ ($A = 48$) orbitals. It is interesting to note that the IMSRG results shown in Fig. 3 agree with the IS + IV Skyrme results based on the $p$-wave form of the interaction. The dependence of $L$ on the type of spin-orbit potential could be resolved by a measurement of the $R_{np}$ of $^{48}$Ca compared to our results for the $A = 36$ and $A = 38$ pairs. The $\Delta R_{ch}$ for the $^{50}$Ni -$^{50}$Ti, $^{52}$Ni -$^{52}$Cr, and $^{54}$Ni -$^{54}$Fe pairs will provide similar information as the $R_{np}$ of $^{48}$Ca [7,8].

## V. CONCLUSION

Our IMSRG calculations fall into a narrow range of values for $\Delta R_{ch}$ and $L$. We stress that these results are predictions, because the parameters of the underlying family of chiral $NN$ plus $3N$ interactions have been determined completely in $A \leqslant 4$ nuclei. While absolute charge radii vary by $\pm 5\%$ compared

to experiment, with the interaction cutoffs, the predictions for $\Delta R_{\rm ch}$ vary only weakly. The EM1.8/2.0 interaction, which is empirically successful for energies up to $A = 60$ (see Ref. [35]), predicts a $\Delta R_{\rm ch}(A = 36)$ within one sigma of the experimental value. This indicates the viability of using differential observables like $\Delta R_{\rm ch}$ to test and possibly constrain next-generation chiral interactions, although more work on quantifying the theoretical uncertainties of IMSRG and other *ab initio* approaches is still required. The lowest value of $\Delta R_{\rm ch}$ ($A = 36$) obtained with EM1 1.8/2.0 agrees with the upper range of the experimental (one sigma) error band.

The Skyrme with the isoscalar spin-orbit form and the CODF provide consistent results with $L$ being constrained to the range $L = 15$–$70$ MeV. The addition of an isovector spin-orbit potential for Skyrme would move the lower limit to $L = 5$ MeV. The present result is about a factor of 3 more precise than the value of $L$ deduced from the PREX [9,47,48] as shown in Figs. 1 and 2. Our range is consistent with the range of $L$ of 11–65 MeV deduced from the observation of the gravitational-wave event of the neutron star merger GW170817 [49]. This rules out a significant number of calculations that have $L > 70$.

## VI. SUMMARY

The $\Delta R_{\rm ch}$ between mirror nuclei were evaluated for the $^{36}$Ca -$^{36}$S and $^{38}$Ca -$^{38}$Ar mirror pairs. The results were compared with theoretical predictions based on the Skyrme EDFs, the CODF theory, and the IMSRG approach. The $\Delta R_{\rm ch}$ and $L$ correlation implies a constraint on $L$ as $5 \leqslant L \leqslant 70$ MeV. This range can be slightly reduced if the ambiguity in the form of the spin-orbit potential could be removed, which can be done by comparing the $\Delta R_{\rm ch}$ for $A = 36, 38$ with neutron skin of $^{48}$Ca.

## ACKNOWLEDGMENTS

We thank C. Drischler for sending us the numerical values of $L$ for the chiral forces used in this work, and K. Hebeler for providing momentum space inputs for the production of interaction matrix elements. This work was supported in part by the National Science Foundation under Grants No. PHY-15-65546, No. PHY-18-11855, and No. PHY-19-13509; the U.S. Department of Energy, National Nuclear Security Administration, Grant No. DE-NA0002924; the U.S. Department of Energy, Office of Science, Office of Nuclear Physics, Grants No. DE-AC05-00OR22725 with UT-Battelle, LLC, No. DE-FG02-92ER40750, No. DE-SC0017887, and the NUCLEI2 SCiDAC4 Collaboration Grant No. DE-SC0018083; Natural Sciences and Engineering Research Council of Canada under Grant No. SAPPJ-2017-00039; and the Deutsche Forschungsgemeinschaft through Grant No. SFB 1245.

[1] B. A. Brown, Phys. Rev. Lett. **85**, 5296 (2000).
[2] D. Steppenbeck, S. Takeuchi, N. Aoi, P. Doornenbal, M. Matsushita, H. Wang, H. Baba, N. Fukuda, S. Go, M. Honma *et al.*, Nature (London) **502**, 207 (2013).
[3] C. J. Horowitz and J. Piekarewicz, Phys. Rev. Lett. **86**, 5647 (2001).
[4] B. P. Abbott *et al.* (The LIGO Scientific Collaboration and the Virgo Collaboration), Phys. Rev. Lett. **119**, 161101 (2017).
[5] B. P. Abbott *et al.* (The LIGO Scientific Collaboration and the Virgo Collaboration), Phys. Rev. Lett. **121**, 161101 (2018).
[6] P. G. Reinhard and W. Nazarewicz, Phys. Rev. C **93**, 051303(R) (2016).
[7] B. A. Brown, Phys. Rev. Lett. **119**, 122502 (2017). The results in this Letter were obtained with the scalar plus isovector form of the Skyrme spin-orbit potential.
[8] J. Yang and J. Piekarewicz, Phys. Rev. C **97**, 014314 (2018).
[9] S. Abrahamyan, Z. Ahmed, H. Albataineh, K. Aniol, D. S. Armstrong, W. Armstrong, T. Averett, B. Babineau, A. Barbieri, V. Bellini *et al.*, Phys. Rev. Lett. **108**, 112502 (2012).
[10] P.-G. Reinhard and W. Nazarewicz, Phys. Rev. C **81**, 051303(R) (2010).
[11] J. Piekarewicz, B. K. Agrawal, G. Colò, W. Nazarewicz, N. Paar, P.-G. Reinhard, X. Roca-Maza, and D. Vretenar, Phys. Rev. C **85**, 041302(R) (2012).
[12] A. Tamii, I. Poltoratska, P. von Neumann-Cosel, Y. Fujita, T. Adachi, C. A. Bertulani, J. Carter, M. Dozono, H. Fujita, K. Fujita *et al.*, Phys. Rev. Lett. **107**, 062502 (2011).
[13] D. M. Rossi, P. Adrich, F. Aksouh, H. Alvarez-Pol, T. Aumann, J. Benlliure, M. Böhmer, K. Boretzky, E. Casarejos, M. Chartier *et al.*, Phys. Rev. Lett. **111**, 242503 (2013).
[14] P. Campbell, I. D. Moore, and M. R. Pearson, Prog. Part. Nucl. Phys. **86**, 127 (2016).
[15] A. J. Miller, K. Minamisono, A. Klose, D. Garand, C. Kujawa, J. D. Lantis, Y. Liu, B. Maaß, P. F. Mantica, W. Nazarewicz *et al.*, Nat. Phys. **15**, 432 (2019).
[16] G. Fricke and K. Heilig, *Nuclear Charge Radii* (Springer, Berlin/Heidelberg, 2004).
[17] R. C. Barrett, Phys. Lett. B **33**, 388 (1970).
[18] L. A. Schaller, D. A. Barandao, P. Bergem, M. Boschung, T. Q. Phan, G. Piller, A. Ruetschi, L. Schellenberg, H. Schneuwly, G. Fricke *et al.*, Phys. Rev. C **31**, 1007 (1985).
[19] B. A. Brown, Phys. Rev. Lett. **111**, 232502 (2013).
[20] C. Y. Tsang, B. A. Brown, F. J. Fattoyev, W. G. Lynch, and M. B. Tsang, Phys. Rev. C **100**, 062801(R) (2019).
[21] G. A. Lalazissis, J. Konig, and P. Ring, Phys. Rev. C **55**, 540 (1997).
[22] G. A. Lalazissis, S. Raman, and P. Ring, At. Data Nucl. Data Tables **71**, 1 (1999).
[23] B. G. Todd-Rutel and J. Piekarewicz, Phys. Rev. Lett. **95**, 122501 (2005).
[24] F. J. Fattoyev, C. J. Horowitz, J. Piekarewicz, and G. Shen, Phys. Rev. C **82**, 055803 (2010).
[25] F. J. Fattoyev and J. Piekarewicz, Phys. Rev. Lett. **111**, 162501 (2013).
[26] W.-C. Chen and J. Piekarewicz, Phys. Rev. C **90**, 044305 (2014).
[27] W.-C. Chen and J. Piekarewicz, Phys. Lett. B **748**, 284 (2015).
[28] T. Niksic, D. Vretenar, and P. Ring, Prog. Part. Nucl. Phys. **66**, 519 (2011).
[29] H. Hergert, Phys. Scr. **92**, 023002 (2017).

[30] H. Hergert, S. K. Bogner, T. D. Morris, A. Schwenk, and K. Tsukiyama, Phys. Rep. **621**, 165 (2016), memorial volume in honor of Gerald E. Brown.
[31] H. Hergert, S. K. Bogner, T. D. Morris, S. Binder, A. Calci, J. Langhammer, and R. Roth, Phys. Rev. C **90**, 041302(R) (2014).
[32] K. Hebeler, S. K. Bogner, R. J. Furnstahl, A. Nogga, and A. Schwenk, Phys. Rev. C **83**, 031301(R) (2011).
[33] C. Drischler, K. Hebeler, and A. Schwenk, Phys. Rev. Lett. **122**, 042501 (2019).
[34] J. Simonis, S. R. Stroberg, K. Hebeler, J. D. Holt, and A. Schwenk, Phys. Rev. C **96**, 014303 (2017).
[35] J. D. Holt, S. R. Stroberg, A. Schwenk, and J. Simonis, arXiv:1905.10475.
[36] E. Tiesinga, P. J. Mohr, D. B. Newell, and B. N. Taylor, the 2018 CODATA recommended values for the fundamental physical constants, http://physics.nist.gov/constants.
[37] M. Tanabashi *et al.* (Particle Data Group), Phys. Rev. D **98**, 030001 (2018).
[38] R. Pohl, A. Antognini, F. Nez, F. D. Amaro, F. Biraben, J. M. R. Cardoso, D. S. Covita, A. Dax, S. Dhawan, L. M. P. Fernandes *et al.*, Nature (London) **466**, 213 (2010).
[39] N. Berginov, T. Valdez, M. Horbatsch, A. Marsman, A. C. Vutha, and E. A. Hessels, Science **365**, 1007 (2019).
[40] A. Beyer, L. Maisenbacher, A. Matveev, R. Pohl, K. Khabarova, A. Grinin, T. Lamour, D. C. Yost, T. W. Hänsch, N. Kolachevsky, and T. Udem, Science **358**, 79 (2017).
[41] W. Xiong, A. Gasparian, H. Gao, D. Dutta, M. Khandaker, N. Liyanage, E. Pasyuk, C. Peng, X. Bai, L. Ye *et al.*, Nature (London) **575**, 147 (2019).
[42] C. J. Horowitz and J. Piekarewicz, Phys. Rev. C **86**, 045503 (2012).
[43] A. Ong, J. C. Berengut, and V. V. Flambaum, Phys. Rev. C **82**, 014320 (2010).
[44] D. Vautherin and D. M. Brink, Phys. Rev. C **5**, 626 (1972).
[45] M. M. Sharma, G. Lalazissis, J. Konig, and P. Ring, Phys. Rev. Lett. **74**, 3744 (1995).
[46] P. G. Reinhard and H. Flocard, Nucl. Phys. A **584**, 467 (1995).
[47] C. J. Horowitz, Z. Ahmed, C. M. Jen, A. Rakhman, P. A. Souder, M. M. Dalton, N. Liyanage, K. D. Paschke, K. Saenboonruang, R. Silwal *et al.*, Phys. Rev. C **85**, 032501(R) (2012).
[48] X. Roca-Maza, M. Centelles, X. Viñas, and M. Warda, Phys. Rev. Lett. **106**, 252501 (2011).
[49] C. A. Raithel and F. Özel, Astrophys. J. **885**, 121 (2019).